

Bottom-Up Statistical PLC Channel Modeling - Part I: Random Topology Model and Efficient Transfer Function Computation

Andrea M. Tonello, *Member, IEEE*, and Fabio Versolatto, *Graduate Student Member, IEEE*

Abstract—We propose an efficient bottom-up power line communication (PLC) channel simulator that exploits transmission line theory concepts and that is able to generate statistically representative in-home channels. We first derive from norms and practices a statistical model of European in-home topologies. The model describes how outlets are arranged in a topology and are interconnected via intermediate nodes referred to as derivation boxes. Then, we present an efficient method to compute the channel transfer function (CTF) between any pair of outlets belonging to a topology realization. The method is based on a systematic remapping technique that leads to the subdivision of the network in elementary units, and on an efficient way to compute the unit transfer function referred to as voltage ratio approach.

The difference from the more conventional and complex ABCD matrix approach is also discussed. We finally show that the simulator can be configured with a small set of parameters and that it offers a theoretical framework to study the statistical PLC channel properties as a function of the topology characteristics, which is discussed in Part II of this work.

Index Terms—Power line communications, channel modeling, in-home networks.

I. INTRODUCTION

NOWADAYS power lines are employed not only for power delivery but they are also becoming an attractive mean for data transmission both in outdoor and indoor scenarios due to their widespread presence. Since power lines have been designed for power delivery, they are a hostile media for communications. Latest transmission techniques, such as multicarrier schemes, overcome most of the criticalities, ensuring communications even for channels with high attenuation and frequency selective fading effects. The design of these advanced communication systems requires the knowledge of the channel characteristics and the use of a model. Although there exist several deterministic channel simulators, very little work has been done to develop a statistically representative model.

Deterministic channel modeling can follow either a top-down or a bottom-up approach. The former handles the power line channel as a black box and returns an analytical expression of its response by fitting results from measurements accounting for multipath propagation in the time domain, via the so-called “echo model” [1], [2], or in the frequency domain

[3]. This approach allows fast channel simulations, but it lacks strong connection with physical reality. Conversely, the bottom-up approach yields the channel transfer function exploiting transmission line (TL) theory under the transverse electromagnetic (TEM) or quasi TEM propagation assumption. It ensures strong connection with physical reality since it uses all the topological information of the network. Both time domain and frequency domain bottom-up approaches have been proposed. The former exploits the multipath propagation model and it describes all the reflection effects encountered by the transmitted signal [4]. The latter tackles the same propagation problem in the frequency domain with a calculation method that uses the ABCD [5], [6] or the scattering matrices [7].

Statistical PLC channel modeling is also of great importance because it allows the design of transmission techniques and their performance analysis. Statistical top-down channel models have been proposed in [8] where an analytical formulation is followed, and in [9] where the results of an experimental campaign presented in [10] are exploited. On the contrary, in this paper we follow a bottom-up approach where the CTF is obtained applying TL theory to realizations of a network topology. Two main issues arise with this approach. Firstly, the need of deriving a statistically representative topology model. Secondly, the derivation of an efficient method to compute the CTF since this task can be computationally intense for complex networks. A similar approach has been presented in [6] which however targets the American indoor scenario satisfying the National Electric Code (NEC) wiring norms.

In this paper, we first present, in Section II, a novel random indoor topology model that has been derived from the observation of in-home European wiring practices and norms. The model describes how outlets are arranged in a topology and are interconnected via intermediate nodes referred to as derivation boxes. Then, in Section III, we provide an efficient CTF computation methodology that we refer to as voltage ratio approach. It was firstly presented in [11]. Herein, we summarize the main relations and we use them, in the Appendix, to discuss the differences with the more common ABCD matrix method. We also describe a three p.u.l. parameters model for the description of the power line cables. In Section IV, we report a numerical example.

The proposed statistical PLC channel simulator is a powerful tool that allows fast generation of CTFs, yet keeping connection with physical reality. It provides a theoretical framework to infer the channel statistical characteristics. To

Manuscript received February 17, 2010; revised May 6, 2010 and August 24, 2010; accepted October 23, 2010.

The authors are with the Dipartimento di Ingegneria Elettrica, Gestionale e Meccanica, DIEGM, Università di Udine, Udine 33100, Italy, (e-mail: tonello@uniud.it; fabio.versolatto@uniud.it).

this respect, some preliminary results of the statistical analysis have been presented in [12] while a more comprehensive study is reported in Part II of this work [13]. Another interesting topic is the comparison between the top-down statistical modeling approach and the bottom-up approach. Some discussion about this aspect has been reported in [14].

II. THE TOPOLOGY MODEL AND GENERATION ALGORITHM

The analysis of European in-home norms and wiring practices reveals that a regular and structured wiring deployment exists, as representatively shown by the layout in Fig. 1. Two connection levels can be usually found. The first one between outlets of a room and the associated derivation box. The second connection level is between the derivation boxes. These connections use dedicated cables, according to reachability and nearness criteria that keep into account the special role played by the main panel connected to the energy supplier network.

Thus, the topology can be divided in area elements that contain all the outlets connected to a derivation box and the derivation box itself. We refer to these area elements as “clusters”. From experimental evidences we have found that clusters have a rectangular shape with a variable dimension ratio, but the same area on average. These observations have allowed us to derive the statistical topology model that we present in the next subsection.

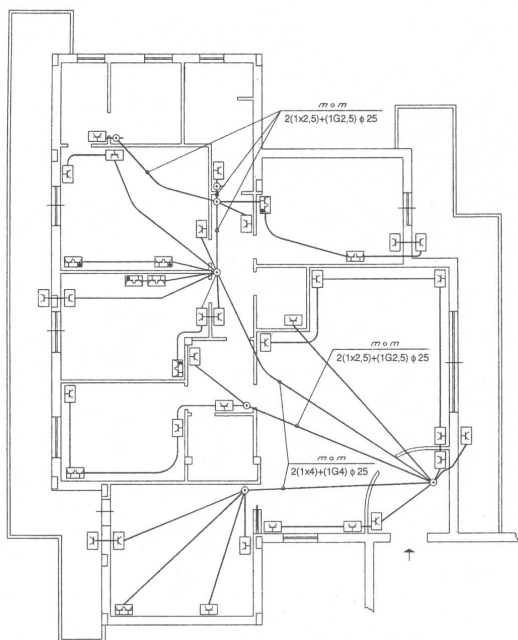


Fig. 1. A typical in-home topology layout showing derivation boxes and connections with outlets.

A. Topology Layout Arrangement

We assume a certain topology area A_f and we divide it into clusters of square shape with identical area A_c . To model the variability of the cluster number and area we consider A_c to be a uniform distributed random variable over a proper

interval, i.e., $A_c \sim \mathcal{U}(A_m, A_M)$, where the minimum and maximum values are determined from experimental evidences, e.g., $A_m = 15 \text{ m}^2, A_M = 45 \text{ m}^2$. It follows that the number of clusters N_c is

$$N_c = \left\lceil \frac{A_f}{A_c} \right\rceil, \quad (1)$$

where $\lceil \cdot \rceil$ denotes the ceiling operator. N_c is a discrete random variable with alphabet $(N_m, N_M) \subset \mathbb{N}$, where

$$A_f/A_m \leq N_M < (A_f + A_m)/A_m, \quad (2)$$

$$A_f/A_M \leq N_m < (A_f + A_M)/A_M. \quad (3)$$

Its probability mass function is

$$P_{N_c}(k) = F_{A_c}(A_f/(k-1)) - F_{A_c}(A_f/k) = \begin{cases} \frac{A_M - A_f}{A_M - A_m} & \text{if } A_f > (k-1)A_M \\ \frac{A_f - A_m}{k-1 - A_m} & \text{if } A_f < kA_m \\ \frac{A_M - A_m}{A_f - A_m} & \text{otherwise} \end{cases} \quad (4)$$

where $F_{A_c}(\cdot)$ is the cumulative distribution function of A_c .

Now, to determine the layout of clusters in the given area we proceed as follows. We define a boolean matrix of size $r \times c$ which represents a regular partition of the area in rc clusters. An element equal to one or zero denotes the presence or absence of the cluster. For example the cluster matrix

$$\mathbf{M} = \begin{bmatrix} 1 & 1 & 1 \\ 1 & 1 & 0 \end{bmatrix}$$

corresponds to the topology layout of Fig. 2.

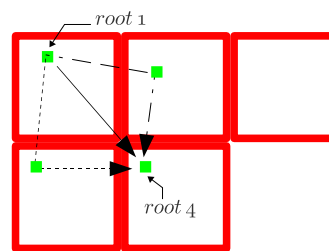


Fig. 2. Example of cluster arrangement and connections between root 1 and root 4.

Furthermore, we model r as a uniformly distributed random variable between 1 and N_c , while the number of columns is $c = \lceil N_c/r \rceil$. Since we want a topology layout of only N_c clusters, when $rc > N_c$, we set to one all elements in the first $r-1$ rows and $c-1$ columns of \mathbf{M} . This is to account for the fact that experimental evidences do not show sparse cluster displacements. Then, we randomly set to zero some elements in the r -th row and c -th column to obtain a total of N_c non-zero elements. The result is a compact topology layout formed by a kernel of $r-1$ by $c-1$ clusters edged by $N_c - (r-1)(c-1)$ additional clusters.

B. Derivation Boxes and Outlets Displacement

From a graph theory perspective, the derivation box can be referred to as “root” of the cluster, since it can be always seen

as the top node of the tree that describes the outlet connections inside the cluster. Usually, roots are regularly spaced and they are not very close to each other. In addition, it can be noted that if two roots are very close, then they can be merged in a unique derivation box which feeds outlets connected to the two initial roots. In our model, the derivation boxes are placed in the top left corner of the associated cluster. To increase the location variability, each derivation box is shifted from its reference corner by a bidimensional offset generated as a pair of uniform distributed random variables defined between 0 and $D = L/4$, where L denotes the cluster side length. More in detail, if we define with (x_r, y_r) the bidimensional offset w.r.t. the cluster edge corner, the final distance from the corner is $d_r = \sqrt{x_r^2 + y_r^2}$, $d_r \in (0, L/2\sqrt{2})$. More in general, under the assumption that the offset coordinates are independent and uniformly distributed in the interval $(0, D)$, the cumulative distribution function of d_r conditioned on D is

$$F_{d_r}(a) = \frac{\pi}{4D^2} a^2 \quad (5)$$

when $0 \leq a < D$, and

$$F_{d_r}(a) = \frac{a^2}{2D^2} \left(\arcsin \frac{D}{a} - \arcsin U(a) \right) + \sqrt{\frac{a^2 - D^2}{D^2}} \quad (6)$$

when $D \leq a \leq \sqrt{2}D$ where

$$U(a) = \sqrt{\frac{a^2 - D^2}{a^2}}. \quad (7)$$

The connection between derivation boxes (roots) is determined keeping into account the special role played by the main panel, i.e., conventionally the root of the top left cluster associated to the element $\mathbf{M}(1, 1)$. Roots are directly connected to the main panel or to the nearest root in the direction of the main panel. In Fig. 2, we depict all possible connections between the roots of cluster 4 and cluster 1. Since the root connections cannot be cyclic, and since we want to satisfy the minimum distance criterion, we have devised the following algorithm to randomly generate the connections.

Firstly, we define an extended cluster matrix as follows

$$\hat{\mathbf{M}} = \begin{bmatrix} 0 & \mathbf{0}_c \\ \mathbf{0}_r & \mathbf{M} \end{bmatrix}, \quad (8)$$

where $\mathbf{0}_c$ and $\mathbf{0}_r^T$ are row vectors with zero elements of size c and r , respectively. We denote the transposition with the T apix. Then, we consider all the possible sub matrices \mathbf{M}_2 of size 2×2 extracted from $\hat{\mathbf{M}}$. For each sub matrix \mathbf{M}_2 , if $\mathbf{M}_2(2, 2)$ is nonzero, then its root is connected to the root of cluster $\mathbf{M}_2(1, 1)$ if this cluster exists, otherwise it is randomly connected to one of the roots of clusters $\mathbf{M}_2(1, 2)$, $\mathbf{M}_2(2, 1)$.

If $\mathbf{M}_2(1, 1)$, $\mathbf{M}_2(1, 2)$ and $\mathbf{M}_2(2, 1)$ are zero, then $\mathbf{M}_2(2, 2)$ is the main panel. The connections between $\mathbf{M}_2(1, 1)$ and $\mathbf{M}_2(2, 2)$ can be done along the diagonal thus with minimum distance, through the root on the top adjacent cluster $\mathbf{M}_2(1, 2)$, or through the root in the left cluster $\mathbf{M}_2(2, 1)$. The second and third solution are still direct connections between $\mathbf{M}_2(1, 1)$ and $\mathbf{M}_2(2, 2)$, and they can be used if adjacent clusters exist.

The outlets are placed along the cluster perimeter according to a Poisson arrival process. This means that the number of outlets is a Poisson variable with alphabet $\mathbb{A} = 1, 2, \dots$ and mean $\Lambda_o A_c$ that increases with the cluster area. The outlet inter-distances are exponentially distributed, and under the condition of a given number of outlets, the outlets are uniformly distributed along the perimeter which is a reasonable assumption. The connections with the derivation box can be done in three different ways as sketched in Fig. 3:

- Type *SD*, Fig. 3(a): a Star structure that satisfies the minimum Distance criteria,
- Type *SP*, Fig. 3(b): a Star topology with conductors placed along the Perimeter,
- Type *BP* Fig. 3(c): a Bus topology with conductors placed again along the Perimeter.

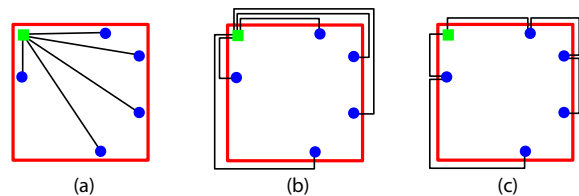


Fig. 3. The three most common connection structures between outlets and root. From left to right, case *SD*, *SP* and *BP*. Squared and dotted markers represent roots and outlets, respectively.

In particular, a widely followed practice suggests to avoid situations where connections form a closed ring around the room. Therefore, we implement this new condition imposing that no connections can cross the corner opposite to the derivation box corner.

With the above model, the length d_l of the connection between an outlet and the derivation box is a random variable whose statistics depend on the connection type. We now report the probability density function (PDF) of d_l conditioned on L and assuming $d_r = 0$. For connections of type *SD*, it reads

$$f_{d_l}(a) = \begin{cases} \frac{1}{2L} & \text{if } 0 \leq a < L, \\ \frac{a}{2L\sqrt{a^2 - L^2}} & \text{if } L \leq a < \sqrt{2}L. \end{cases} \quad (9)$$

When connections are of type *SP*, d_l is a uniform distributed variable

$$f_{d_l}(a) \sim \mathcal{U}(0, 2L). \quad (10)$$

In the presence of a bus topology, d_l is no longer the length of the connection between an outlet and the root, but between an outlet and its neighbor outlet in the direction of the root. For this latter case, the PDF is exponential and equal to

$$f_{d_l}(a) = \frac{1}{2L} \left(1 + \frac{(2L - a)\Lambda_o L}{4} \right) e^{-\frac{\Lambda_o L a}{4}} \quad a \in (0, 2L), \quad (11)$$

Finally, the physical connection between outlets and derivation boxes can be done using cables of different type. This allows the use of higher section cables for root interconnections that are supposed to carry higher currents. In other words, the norms on voltage drop limitations can also be taken into account.

C. Load Distribution

In order to fit reality as much as possible, we also consider the contribution of loads. More in detail, from experimental measurements, we have collected a number of loads N_l that are representative of computer transformers, lamps, or other appliances. These loads are randomly selected, hence the probability to pick the k -th load from the previous set is $p_l(k) = 1/N_l$. Now, if we define p_v as the probability that no loads are connected to a plug, then the probability $p_{l|\bar{v}}(k)$ that the k -th load is connected to an outlet o given that an appliance is connected to o is $p_{l|\bar{v}} = (1 - p_v)/N_l$. Note that we set p_v to a certain value according to our experimental observations.

III. CHANNEL TRANSFER FUNCTION COMPUTATION

The computation of the channel transfer function with the bottom-up approach can be a rather computationally intense task for complex networks as the indoor ones. It is of great importance to use an efficient method. Thus, we propose the approach that we have firstly described in [11], that is referred to as voltage ratio approach. We summarize it here for the sake of completeness and to provide all the equations that allow the comparison with the ABCD matrix method.

For a given topology realization and a pair of outlets, the method starts from the identification of the backbone, i.e., the shortest signal path between the transmitter and the receiver nodes. Then, we remap the topology around the backbone and we split the remapped layout into small parts referred to as units. Each unit comprises a portion of the backbone with homogeneous line characteristics, and eventually, a branch connected in parallel at its input. The end units are those associated to the transmitter and the receiver nodes.

Now, it is important to devise a fast way to remap the topology as a function of the backbone associated to a certain transmitter-receiver node pair. We start from the definition of the network adjacency matrix that collects all the network layout information. Then, we firstly trace back the tree layout of the network and we find the ordered sequence of intermediate nodes between each leaf and the root of the tree. We refer to these sequences of nodes as paths. Thus, we assign a path to each outlet. Finally, the backbone between two outlets is determined by the properly ordered set of unique nodes picked from paths associated to the transmitter and receiver nodes. In a similar way, exploiting path information, the entire network can be remapped as branches connected to the backbone.

A. Impedance Carry-back Method

As discussed in the next sub-section, we assume a TEM or quasi-TEM propagation mode. Then, let us consider a line of length l , characteristic impedance Z_C and propagation constant γ , closed into an impedance load Z_L . From TL theory we can compute the equivalent impedance Z_R seen at the line input as follows

$$Z_R = Z_C \frac{Z_L + Z_C \tanh(\gamma l)}{Z_C + Z_L \tanh(\gamma l)} = Z_C \frac{1 + \rho_L e^{-2\gamma l}}{1 - \rho_L e^{-2\gamma l}}, \quad (12)$$

where $\rho_L = (Z_L - Z_C)/(Z_L + Z_C)$, and where in the notation we omit, as throughout the paper, the frequency dependence for simplicity. This relation is useful in the analysis of complex power line networks because it suggests to collapse the branches into their equivalent impedances placed in parallel along the backbone. Therefore, (12) can be directly used if a branch (line segment) connects a backbone node n_b with an outlet o where a load Z_L is plugged in, i.e., we carry back Z_L to n_b . The method can be extended to multilevel branches, i.e., branches that feed more than one outlet. For instance, let us consider Fig. 4(a). We first carry back to node n_2 the impedances of the loads plugged into the outlets o_1 and o_2 . Then, we compute the equivalent impedance at node n_2 as their parallel obtaining the equivalent circuit in Fig. 4(b). We now repeat the procedure to derive an equivalent impedance for node n_1 obtaining the circuit of Fig. 4(c). Finally, we carry back the equivalent branch impedance to the backbone node n_b .

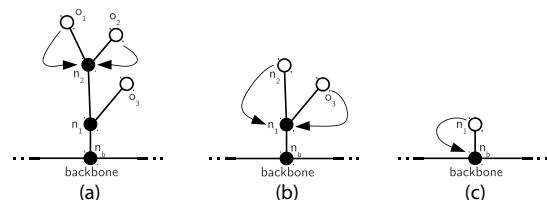


Fig. 4. Three subsequent steps of the impedance carry-back method.

As noted in [11], the carry-back procedure can be significantly simplified (in the sense that is not needed) in the presence of long and non ideal cables, i.e., cables that show a real component for the propagation constant. This is because independently of the load impedance, the input impedance goes to the cable characteristic impedance as the cable length increases. Herein, we show that this conclusion holds true also in the presence of multiple line sections with heterogeneous properties. Let us consider, the simple circuit of Fig. 5.

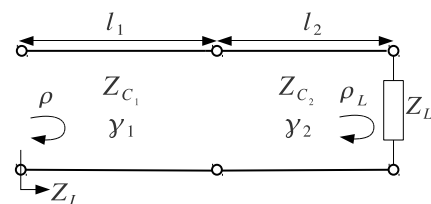


Fig. 5. A simple branch made of two line segments with different electrical properties and closed into a load Z_L .

Applying twice the relation (12) the input impedance can be expressed as

$$Z_I = Z_{C1} \frac{1 + \rho}{1 - \rho} \quad (13)$$

where

$$\rho = \frac{(Z_{C2} + Z_{C1})\rho_L e^{-2\gamma_2 l_2} + (Z_{C2} - Z_{C1})}{(Z_{C2} - Z_{C1})\rho_L e^{-2\gamma_2 l_2} + (Z_{C2} + Z_{C1})} e^{-2\gamma_1 l_1} \quad (14)$$

and $\rho_L = (Z_L - Z_{C2})/(Z_L + Z_{C2})$. Therefore, if l_2 goes to infinity, $\rho_L \exp(-2\gamma_2 l_2)$ vanishes regardless of the load value.

Similarly, we achieve an analogous result if l_1 goes to infinity. In the same manner, if we connect an impedance Z_B at the junction between line 1 and 2 we will find that its contribution to the definition of ρ is scaled at least by $\exp(-2(\gamma_1 l_1))$. In summary, the load does not influence the equivalent branch impedance as long as it is connected to the backbone via long non ideal cables.

B. Voltage Ratio Approach (VRA)

For a topology realization and a given pair of nodes the CTF computation is obtained by firstly finding the backbone and remapping the network topology along it, as described in Section III.A. Then, we collapse the branches into equivalent impedances connected to the backbone. Finally, we compute the CTF as the insertion loss between the transmitter and receiver nodes. Now, if we divide the backbone in $N + 1$ units each with an input node labeled with n_b (towards the transmitter) and output node labeled with n_{b-1} (towards the receiver), the CTF can be computed as the product of the CTF voltage ratio $H_b(f) = V_{b-1}(f)/V_b(f)$ of each unit, that is

$$H(f) = \frac{V_0(f)}{V_{N+1}(f)} = \prod_{b=1}^{N+1} H_b(f). \quad (15)$$

where $V_0(f)$ and $V_{N+1}(f)$ are the measured voltages at the input ports of the receiver and transmitter, respectively, at frequency f .

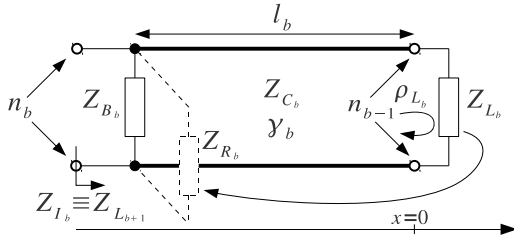


Fig. 6. Elements of a unit belonging to a given backbone.

A given unit b , as depicted in Fig. 6, comprises a portion of the backbone, with homogeneous line characteristics eventually with a branch connected in parallel at its input. In the following, the notation does not explicitly show the frequency dependence. Thus, we refer to Z_{C_b} and γ_b as the characteristic impedance and the propagation coefficient of the backbone line portion of length l_b . In Fig. 6, we also use thick lines to represent physical wires, while thin lines have zero-length and are simply used to graphically represent connections. The equivalent impedance of the branches connected to the node n_b is denoted with Z_{B_b} . By definition, the line segment of each unit connects together two intermediate nodes of the backbone or the last intermediate node to the load Z_L , i.e., the input impedance of the receiver. We set $x = 0$ at node n_{b-1} and we define the load reflection coefficient for unit b as $\rho_{L_b} = (Z_{L_b} - Z_{C_b}) / (Z_{L_b} + Z_{C_b})$.

Hence, we can write the expression for the voltages at nodes n_b and n_{b-1} as

$$V_b = V(e^{\gamma_b l_b} + \rho_{L_b} e^{-\gamma_b l_b}), \quad (16)$$

$$V_{b-1} = V(1 + \rho_{L_b}), \quad (17)$$

respectively, where V is a voltage coefficient that is a function of the boundary conditions, such as the source generator voltage value. Therefore, the unit CTF reads

$$H_b = \frac{V_{b-1}}{V_b} = \frac{1 + \rho_{L_b}}{e^{\gamma_b l_b} + \rho_{L_b} e^{-\gamma_b l_b}}. \quad (18)$$

Now, we need to compute the reflection coefficient ρ_{L_b} . When $b = 1$ this is a trivial task, since Z_{L_b} is the receiver input impedance. Conversely, when $b > 1$, Z_{L_b} is the input impedance of the unit of index $b - 1$, and its computation involves again the impedance carry-back method. More in detail, to estimate the input impedance of the generic unit b shown in Fig. 6, we carry back the load impedance Z_{L_b} up to the input port, according to (12). Then, we compute the parallel of Z_{R_b} and Z_{B_b} and the result yields Z_{I_b} , i.e. the input impedance of the unit b .

It should be noted that the VRA requires to start from the receiver side due to the implicit dependence of (18) from the downstream input impedances.

The key aspect of the proposed method consists in splitting the overall complex problem into $N + 1$ simpler subproblems each of which comprises the computation of the insertion loss and the input impedance of each backbone unit. Note also that the VRA, unlike other well-known methods—such as the ABCD matrix method—handles only scalar quantities and this gives an advantage in terms of computational effort. The relation to the ABCD method is discussed in the Appendix.

C. Line Parameters

Line parameters and cable models play an important role in the computation of the channel transfer function via the bottom-up approach. Different models have been presented in the literature to describe different cable types, such as NYY, NYM or VVF, e.g., in [15], [16] and [17]. These models are widely used to describe the scenarios of countries where norms suggest the deployment of compact cables for in-home wiring. In compact cables both the safety ground wire and the power supply wires, namely phase and neutral, are enclosed into a PVC cap, so they always run closed together. This latter feature ensures the TEM or quasi-TEM propagation. Other layouts comprise single wires displaced in a plastic raceway. Due to the regular structure and the small dimension of the raceway compared to the signal wavelength, the TEM or quasi-TEM propagation mode can still be assumed. Consequently, we use a concentrated parameters model since the radiated field is supposed to be a minor factor [18]. We then define the skin depth as [19]

$$\delta = \frac{1}{\sqrt{\pi \mu f \sigma}}, \quad (19)$$

where μ and σ are respectively the magnetic permeability and the conductivity of the wire, while f is the frequency. We omit the frequency dependence for notation simplicity. We choose the vacuum magnetic permeability equal to $4\pi \cdot 10^{-7} \text{ H/m}$ and the copper conductivity equal to $5.8 \cdot 10^7 \text{ S/m}$. Then, we define r and d as the conductor radius and the distance between conductors, respectively. Finally, we compute the per

unit-length (p.u.l.) resistance R as

$$R = \frac{1}{\pi\sigma r^2} \quad \text{when } \delta \gg r, \quad (20)$$

$$R = \frac{1}{2\pi\sigma r\delta} \quad \text{when } \delta \ll r, \quad (21)$$

and the p.u.l. inductance L as

$$L = \frac{\mu}{\pi} \log\left(\frac{d}{r}\right) + \frac{\mu}{8\pi} \quad \text{when } \delta \gg r, \quad (22)$$

$$L = \frac{\mu}{\pi} \log\left(\frac{d}{r}\right) + \frac{1}{4\pi r} \sqrt{\frac{\mu}{\pi\sigma f}} \quad \text{when } \delta \ll r. \quad (23)$$

If the two conductors are surrounded by an homogeneous dielectric insulator, it can be demonstrated that [18]

$$LC = \mu\varepsilon, \quad (24)$$

that is, the product of the p.u.l. inductance L with the p.u.l. capacitance C is always equal to product of the magnetic permeability with the dielectric constant. For the sake of simplicity, we neglect the presence of inhomogeneous dielectric between the two wires, hence we exploit (24) to obtain the p.u.l. capacitance. In particular, we assume the insulator to be PVC, whose relative dielectric constant ε_r is equal to 3.6, [4]. Hence, $\varepsilon = \varepsilon_r\varepsilon_0 = 3.6 \cdot 8.859 \cdot 10^{-12} \text{ F/m}$. We also neglect the p.u.l. conductance contribution G , due to the very high resistivity of the considered insulated material. Thus, the cable model uses three p.u.l. parameters, and we can compute the characteristic impedance and the propagation constant respectively as

$$Z_C = \sqrt{\frac{R + j2\pi fL}{G + j2\pi fC}} \simeq \sqrt{\frac{R + j2\pi fL}{j2\pi fC}}, \quad (25)$$

$$\gamma = \sqrt{j2\pi fC(R + j2\pi fL)}. \quad (26)$$

IV. CHANNEL SIMULATOR

Following the proposed statistical topology model and CTF computation method we have developed a statistical channel simulator. The simulator uses a small set of parameters that comprises the topology area, the minimum and maximum cluster size, the intensity of outlets per square meter, and the probability of having an open outlet. For simplicity, the cable types and the set of load impedance are pre-computed and stored in a look-up table. An example of parameters that have been used to obtain results in good agreement with experimental campaigns, e.g., [20], is reported in Table I.

TABLE I
SETUP OF THE CHANNEL GENERATOR PARAMETERS

Parameter	Value
$A_f(m^2)$	160
$A_c(m)$	$\mathcal{U}(15, 45)$
$\Lambda_o(\text{outlets}/m^2)$	0.5
p_v	0.3
N_l	10

The simulator firstly generates a topology realization, e.g., the one shown in Fig. 7. The outlets and roots are represented

by dotted and squared shaped markers, respectively. Then, the tree of the topology realization is derived (see Fig. 8). The main panel is the root in the top left cluster and it is labeled as node 1 in the tree representation of Fig. 8. More in general, roots are numbered walking down to columns of the cluster matrix starting from the left. Hence, node 2 is the root of the cluster $M(2, 1)$, and the generic node $n \leq N_c$ is the root of the cluster $M(n - \lfloor(n-1)/r\rfloor \cdot r, \lfloor(n-1)/r\rfloor + 1)$, where r is the number of rows of the cluster matrix M . Outlets underlie a similar numeration: if n_{o1} is the number of outlets of the first cluster, then these outlets are incrementally numbered in the tree plot from $N_c + 1$ to $N_c + n_{o1}$. In addition, inside each cluster the outlet numeration follows the counterclockwise rule shown in the first cluster of Fig. 7.

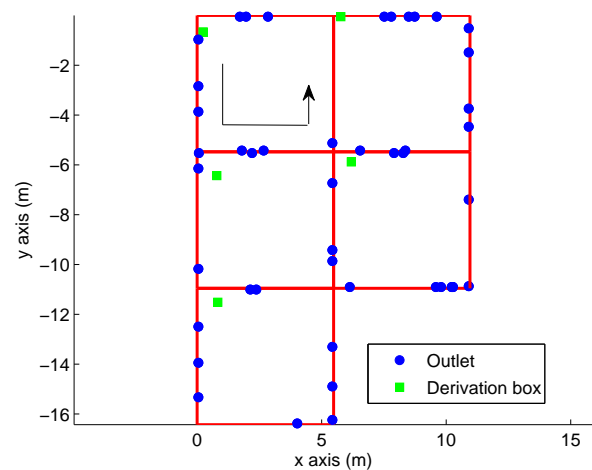


Fig. 7. Layout of the randomly generated topology. the upper left cluster shows the direction followed for the outlet numeration.

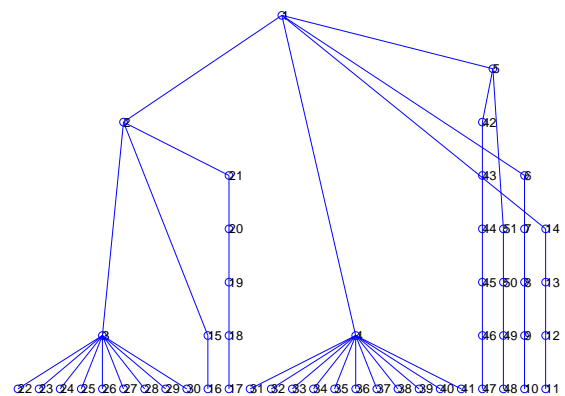


Fig. 8. Tree representation of the generated layout.

We arbitrarily select two pair of outlets, and we compute the corresponding CTF in the 1-30 MHz band with a sampling frequency of 100 kHz. In Fig. 9, we show both the frequency and impulse channel responses. The impulse response is obtained via the inverse Fourier discrete transform (IDFT) of the frequency response. We further smooth the CTF with a raised cosine window.

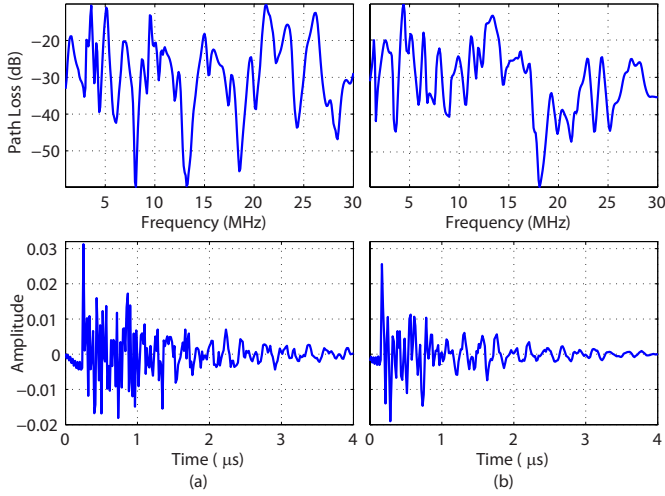


Fig. 9. Frequency and impulse responses of two different channels: (a) between outlets 51 and 23, and (b) between outlets 12 and 27.

An in-depth analysis of the statistical properties of the proposed PLC channel simulator is reported in Part II [13]. We have found a good agreement with the results from measurements campaigns. The simulator is a powerful tool to investigate the properties of the channel keeping connection with physical reality. For instance, it allows inferring the behavior as a function of the topology area, the loads, the outlets distance and the belonging of the outlets to the same or distinct clusters. The generation of time-variant channel responses can also be obtained by including time-variant loads [11]. Moreover, the simulation can be easily extended to the case of multiple homes having nearby located and interconnected main panels, e.g., multiple apartments in a building, by simply connecting together through the main panel different topology realizations. Top-down generators are not yet able to comprehensively offer such information.

V. CONCLUSIONS

In this paper we have presented a statistical bottom-up PLC channel generator for the indoor scenario. We have fully described the topology generation algorithm and a fast channel transfer function computation method. The differences with the ABCD matrix method have also been discussed. The simulator uses a small set of parameters an example of which has been reported. An in-depth statistical analysis of the simulator is carried out in the second part of this work [13] where we show that it is a powerful tool to infer the PLC channel statistics as a function of the topology characteristics. It allows generating statistically representative channels in agreement with experimental measurement campaigns.

APPENDIX A

COMPARISON WITH THE ABCD MATRIX METHOD

Let us consider Fig. 10 which describes the channel backbone between a pair of outlets as the composition of elementary units. From the definitions of Section III, a unit comprises a backbone line segment and a branch. The latter

can always be modeled as an equivalent admittance according to the impedance carry-back method of Section III.B. If we

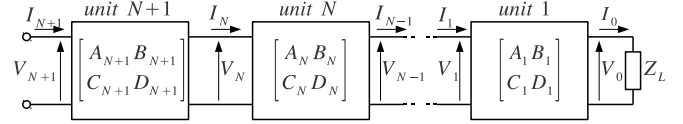


Fig. 10. Structure of a backbone divided in $N + 1$ subunits, each of which is described by its ABCD matrix.

know the ABCD matrix of each unit b

$$\begin{bmatrix} V_b \\ I_b \end{bmatrix} = \begin{bmatrix} A_b & B_b \\ C_b & D_b \end{bmatrix} \begin{bmatrix} V_{b-1} \\ I_{b-1} \end{bmatrix} \quad (27)$$

we can exploit the chain rule to obtain

$$\begin{aligned} \begin{bmatrix} V_{tx} \\ I_{tx} \end{bmatrix} &= \begin{bmatrix} V_{N+1} \\ I_{N+1} \end{bmatrix} = \begin{bmatrix} A_{N+1} & B_{N+1} \\ C_{N+1} & D_{N+1} \end{bmatrix} \\ &\times \begin{bmatrix} A_N & B_N \\ C_N & D_N \end{bmatrix} \cdots \begin{bmatrix} A_1 & B_1 \\ C_1 & D_1 \end{bmatrix} \begin{bmatrix} V_0 \\ I_0 \end{bmatrix}. \end{aligned} \quad (28)$$

However, since each unit comprises the cascade of the equivalent admittance of a branch and a line segment (see also Fig. 6), we can reformulate the ABCD matrix of the b -th unit as

$$\begin{aligned} \begin{bmatrix} A_b & B_b \\ C_b & D_b \end{bmatrix} &= \begin{bmatrix} 1 & 0 \\ Y_{B_b} & 1 \end{bmatrix} \\ &\times \begin{bmatrix} \cosh(\gamma_b l_b) & Z_{C_b} \sinh(\gamma_b l_b) \\ Y_{C_b} \sinh(\gamma_b l_b) & \cosh(\gamma_b l_b) \end{bmatrix}, \end{aligned} \quad (29)$$

that is, the ABCD matrix of the admittance $Y_{B_b} = 1/Z_{B_b}$ multiplied by the ABCD matrix of the backbone line segment which belongs to unit b . We also define $Y_{C_b} = 1/Z_{C_b}$ as the characteristic impedance of the line. Now, let us suppose to know the equivalent load admittance for the b -th unit $Y_{L_b} = I_{b-1}/V_{b-1} = 1/Z_{L_b}$. Then, from (29) the expression of V_b as a function of V_{b-1} reads

$$V_b = (\cosh(\gamma_b l_b) + Z_{C_b} Y_{L_b} \sinh(\gamma_b l_b)) V_{b-1}, \quad (30)$$

where we neglect the dependence from frequency to simplify the notation. In particular, it is worthwhile noting that Y_{L_b} is the receiver input admittance for the unit $b = 1$, and the input admittance of the unit $(b-1)$, otherwise. The previous equation can be further manipulated. To this end, we first define the load reflection coefficient for unit b as

$$\rho_{L_b} = \frac{Y_{C_b} - Y_{L_b}}{Y_{C_b} + Y_{L_b}}. \quad (31)$$

Then, we can express Y_{L_b} as a function of ρ_{L_b} and use this new formulation into (30) to obtain the ratio between V_b and V_{b-1} , i.e., the insertion loss of the b -th unit given by (18). Therefore, we have found the VRA core equation starting from the ABCD matrix description of the network. To compute (18) for every unit b , we need the load impedance of all the units. We can exploit again the impedance carry-back method, to obtain the input admittance of unit b as follows

$$Y_{I_b} = Y_{B_b} + Y_{C_b} \frac{Y_{L_b} + Y_{C_b} \tanh(\gamma_b l_b)}{Y_{C_b} + Y_{L_b} \tanh(\gamma_b l_b)} = Y_{B_b} + Y_{R_b}, \quad (32)$$

where Y_{R_b} is the equivalent load admittance obtained by carrying back Y_{L_b} to the upstream port of unit b . Starting from unit $b = 1$, we can recursively apply (32) to compute the load impedance, and consequently the insertion loss, for each unit b . Finally, the overall insertion loss is the product of the individual unit insertion losses according to (15).

In conclusion, while the ABCD matrix method exploits the chain rule to obtain an overall ABCD matrix which gathers and merges all the information about the system, the voltage ratio approach splits up the analysis in a certain number of sub-units for which it computes the input admittance and the insertion loss. The VRA can be thought as a scalar version of the ABCD matrix method since it handles only scalar elements which allows lowering the implementation complexity.

REFERENCES

- [1] L. T. Tang, P. L. So, E. Gunawan, Y. L. Guan, S. Chen, and T. Lie, "Characterization and Modeling of In-Building Power Lines for High-Speed Data Transmission," *IEEE Trans. Power Del.*, vol. 18, no. 1, pp. 69–77, Jan. 2003.
- [2] H. Phillips, "Modelling of Powerline Communication Channels," in *Proc. IEEE Int. Symp. Power Line Commun. and its App.*, Mar. 1999, pp. 14–21.
- [3] M. Zimmermann and K. Doster, "A Multipath Model for the Powerline Channel," *IEEE Trans. Commun.*, vol. 50, no. 4, pp. 553–559, Apr. 2002.
- [4] I. C. Papaleonidopoulos, C. G. Karagiannopoulos, I. E. Anagnostopoulos, and N. J. Theodorou, "An HF Multipath-Propagation Analysing Method for Power Delay Profile Estimations of Indoor Single Phase Low Voltage PLC Channels," in *Proc. IEEE Int. Symp. Power Line Commun. and its App.*, Mar. 2003, pp. 154–159.
- [5] S. Galli and T. C. Banwell, "A Deterministic Frequency-Domain Model for the Indoor Power Line Transfer Function," *IEEE J. Sel. Areas Commun.*, vol. 24, no. 7, pp. 1304–1316, Jul. 2006.
- [6] T. Esmalian, F. R. Kschischang, and P. Glenn Gulak, "In-building Power Lines as High-Speed Communication Channels: Channel Characterization and a Test Channel Ensemble," *International Journal of Communication Systems*, vol. 16, pp. 381–400, 2003.
- [7] H. Meng, Y. L. Guan, C. L. Law, P. L. So, E. Gunawan, and T. Lie, "Modeling of Transfer Characteristics for the Broadband Power Line Communication Channel," *IEEE Trans. Power Del.*, vol. 19, no. 3, pp. 1057–1064, Jul. 2004.
- [8] A. M. Tonello, "Wideband Impulse Modulation and Receiver Algorithms for Multiuser Power Line Communications," *EURASIP Journal on Advances in Signal Processing*, vol. 2007, Article ID 96747, 14 pages, 2007. doi:10.1155/2007/96747.
- [9] M. Tlich, A. Zeddani, A. Moulin, F. Gauthier, and G. Avril, "A Broadband Powerline Channel Generator," in *Proc. IEEE Int. Symp. Power Line Commun. and its App.*, Mar. 2007, pp. 505–510.
- [10] M. Tlich, A. Zeddani, A. Moulin, and F. Gauthier, "Indoor Power-Line Communications Channel Characterization up to 100 MHz—Part I: One-Parameter Deterministic Model," *IEEE Trans. Power Del.*, vol. 23, no. 3, pp. 1392–1401, July 2008.
- [11] A. M. Tonello and T. Zheng, "Bottom-Up Transfer Function Generator for Broadband PLC Statistical Channel Modeling," in *Proc. IEEE Int. Symp. Power Line Commun. and its App.*, Apr. 2009, pp. 7–12.
- [12] F. Versolatto and A. M. Tonello, "Analysis of the PLC Channel Statistics Using a Bottom-Up Random Simulator," in *Proc. IEEE Int. Symp. Power Line Commun. and its App.*, Mar. 2010, pp. 236–241.
- [13] A. M. Tonello and F. Versolatto, "Bottom-Up Statistical PLC Channel Modeling - Part II: Inferring the Statistics," *IEEE Trans. Power Del.*, vol. 25, no. 4, pp. 2356–2363, Oct. 2010.
- [14] A. M. Tonello and F. Versolatto, "New Results on Top-Down and Bottom-Up Statistical PLC Channel Modeling," in *Third Workshop on Power Line Commun. and its App.*, Oct. 2009, pp. 11–14.
- [15] I. C. Papaleonidopoulos, C. G. Karagiannopoulos, N. J. Theodorou, and C. N. Capsalis, "Theoretical Transmission-Line Study of Symmetrical Indoor Triple-Pole Cables for Single-Phase HF Signalling," *IEEE Trans. Power Del.*, vol. 20, no. 2, pp. 646–654, Apr. 2005.
- [16] I. C. Papaleonidopoulos, C. G. Karagiannopoulos, N. J. Theodorou, I. E. Anagnostopoulos, and C. E. Anagnostopoulos, "Modeling of Indoor Low Voltage Power-Line Cables in the High Frequency Range," in *Proc. IEEE Int. Symp. Power Line Commun. and its App.*, Mar. 2002, pp. 267–271.
- [17] S. Tsuzuki, T. Takamatsu, H. Nishio, and Y. Yamada, "An Estimation Method of the Transfer Function of Indoor Power-Line Channels for Japanese Houses," in *Proc. IEEE Int. Symp. Power Line Commun. and its App.*, Mar. 2002, pp. 55–59.
- [18] R. P. Clayton, *Analysis of Multiconductor Transmission Lines*. Wiley-IEEE Press, Nov. 2007.
- [19] S. Ramo, J. R. Whinnery, and T. Van Duzer, *Fields and Waves in Communication Electronics*. Wiley & Sons, 1994.
- [20] S. Galli, "A Simplified Model for the Indoor Power Line Channel," in *Proc. IEEE Int. Symp. Power Line Commun. and its App.*, Apr. 2009, pp. 13–19.



Andrea M. Tonello is an aggregate professor at the University of Udine, Italy, and the founder of the wireless and power line communication lab (WiPLi Lab). From 1997 to 2002 he was with Bell Labs - Lucent (NJ, USA) first as a Member of Technical Staff and then promoted to Technical Manager, and Managing Director of Bell Labs, Italy. He received an EURASIP best journal paper award in 2007, and he was the co-author of the best student paper award at IEEE International Symposium on Power Line Communications (ISPLC) 2010 both about PLC. Dr.

Tonello is the vice-chair elected of the IEEE Technical Committee on Power Line Communications. He is the chair of IEEE ISPLC 2011, Udine Italy. More details can be found in Part II of this paper.



Fabio Versolatto received the Laurea degree in 2007 and the Laurea Specialistica degree in electrical engineering in 2009 (both cum laude) from the University of Udine, Italy. Currently he is working towards the Ph.D. at the University of Udine. His research interests are about PLC channel modeling and digital communication algorithms. He received the award for the best student paper presented at IEEE ISPLC 2010.